



11th Global Conference on Sustainable Manufacturing

2013

23rd - 25th September
Berlin - Germany

8.5 A thermal analysis framework for cryogenic machining and its contribution to product and process sustainability

T. Lu, O. W. Dillon, Jr., I. S. Jawahir

Institute for Sustainable Manufacturing (ISM), University of Kentucky, Lexington, USA

Abstract

Cryogenic processing methods are environmentally-clean, toxic-free, and safe sustainable manufacturing processes, which also provide improved surface integrity, superior functional performance and greater product life in manufacturing processes. This paper presents a summary of findings from a preliminary study of the cryogenic cooling effects in a machining process. Various heat transfer scenarios need to be built into the model to consider the boiling phenomena. Cryogenic turning process includes a large radial thermal gradient in a thin layer of machined surface and changes the dynamic recrystallization process. A high speed, wide range temperature measurement system was developed, and preliminary experiments are carried out, investigating the contributing factors and the proper boundary conditions for modeling of cryogenic machining processes. The transition from slow cooling to a rapid cooling is observed.

Keywords:

Product/process sustainability, Cryogenic machining, Cooling, Boiling, Boundary conditions

1 INTRODUCTION

The most prominent issue in machining processes is the abundant, and often indiscriminate use of cutting fluids (CFs). Despite their anticipated benefits of better tool-life, better product quality and better chip evacuation, CFs overall have a negative impact on the economic performance of the process, the machine operators and the environment. The cost involved in the application of CFs is not limited to the purchased price paid, but also includes the cost involved in coolant system maintenance and treatment of used CFs, which takes up to 16% of the total machining cost [1][2]. Disposal of used CFs and emissions from the CF applications have potential hazardous impact on the environment. Contacting CFs and inhaling the airborne particles from coolant application could cause several different diseases [3].

These problems have over the years motivated researchers to find alternative techniques such as dry machining (cutting with no CFs) and minimal quantity of lubrication (MQL) machining. However, these more sustainable options can hardly provide sufficient cooling capability to replace the conventional CFs.

The cryogenic machining, which involves the use of cryogenic fluids such as the liquid nitrogen, is a competitive alternative. To make cryogenic machining a truly sustainable process, one must apply the coolant appropriately considering its cost and the embedded energy. While the sustainability performance of such a process could be assessed by a sustainability evaluation methodology [4][5], the parameter optimization requires a proper modeling of the process.

Despite its growing popularity in machining applications, in spite of the perceived difficulties in justifying the cost effectiveness, the exact cooling behavior due to cryogenic fluid application during the machining is not adequately understood. There is little known about the optimal use of cryogenic conditions for energy efficiency, operational effectiveness, product and process quality in terms of

sustainability, etc. This paper presents a framework of heat transfer analysis of cryogenic machining from the sustainable manufacturing viewpoint. The fundamental theories of boiling heat transfer are introduced, followed by an experimental investigation applying high speed temperature measurement. Preliminary experimental results are shown to offer promising guidelines for future work.

With a proper understanding of the cooling effect in cryogenic machining, one could properly determine the optimal condition, including process parameters, coolant flow parameters and machine tool requirements, which would lead to optimized sustainability performance of the process regarding economic, environment and societal aspects.

2 BACKGROUND

2.1 Heat transfer in machining processes

Tool-life will heavily depend on the tool temperature [6], since high tool temperature usually leads to rapid tool-wear. Also, the high temperature of machined workpiece may have a negative impact on the product quality, such as softened material and poor accuracy. Many materials may show dynamic recrystallization during machining process [7]. This dynamic recrystallization will generate a surface layer with fine grains, which may be beneficial to the quality and performance of the manufactured product, ultimately producing more sustainable products. However, the high temperature on the workpiece surface in the machining process may activate grain growth, thus reduce or even eliminate the grain refinement effect. Therefore, it is very important to efficiently remove the heat generated in the machining process.

Heat transfer analysis due to cutting fluid applications in machining processes has been carried out by many researchers, such as Yue et al. [8] and Sun et al. [9]. These researchers considered conduction and convection heat transfer, and their focus has been on the fluid dynamics

around the cutting zone, including the rake and the flank regions [10]. In this paper, the focus is on the coolant application on the flank region, as it is considered most relevant to the dynamic recrystallization and grain growth suppression in the machined surface layer.

The temperature distributions in cryogenic machining were measured experimentally by embedding thermocouples into the workpiece or cutting tools [11]. The focus was on the material behavior and the cutting tool performance under cryogenic conditions, while the cooling effect is taken as a convection heat transfer process with a similar heat transfer coefficient as conventional flood cooling.

2.2 Boiling heat transfer

The saturation temperature of liquid nitrogen is -196°C at the pressure of one Bar (about 0.1MPa). Severe phase change, known as boiling, will occur when liquid nitrogen contacts the workpiece and the cutting tool, which may be at or above the room temperature. In practices, liquid nitrogen is usually stored in pressurized tanks. When released from pressurized vessel, the phase change may occur even before its physical contact with the workpiece and the cutting tool.

The famous Nukiyama Curve describing the boiling heat transfer [12] is shown in Figure 1 [13]. It is suggested that boiling will introduce a greater heat flux compared to convection heat transfer. Critical heat flux is reached when the vapor begins to cover the surface and to decrease the cooling efficiency.

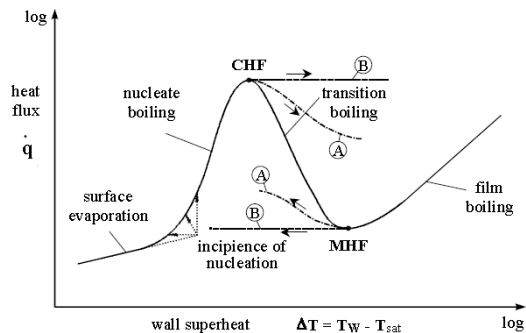


Figure 1: The Nukiyama Curve [13].

Such boiling heat transfer scenarios are well-studied in the field of controlled cooling of rolled metals. Some of the reported heat transfer data of hot plate cooled by water jets suggest surface heat transfer coefficient as high as $2 \times 10^5 \text{ W}/(\text{m}^2\text{C})$ and cooling rate of $10 \sim 20 \text{ C/s}$ [14]. Such values are around two orders of magnitude higher than the typical values used and found in other literatures in the machining area.

The time duration of the cutting fluid contact with the workpiece in cryogenic machining is very short compared to the controlled cooling of steel rolling. The exposure duration depends on the machining parameters and the size of the coolant coverage area. Combined with a high surface heat flux during this period, cryogenic application from the flank side would probably leave a shallow, but a much-cooled layer on top of the machined surface. After cooled zone exits the coolant coverage, the heat from the bulk part of the workpiece and the air will heat the cooled zone. The rapid cooling and heat-up processes on the boiling-cooled surface are observed in moving plate cooling experiments [14], as shown in Figure 2.

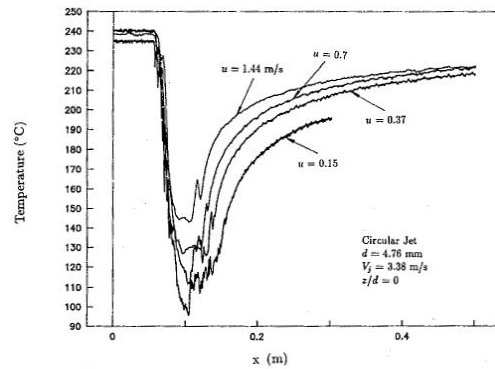


Figure 2: Measured plate surface temperature [14].

The control parameters influencing the heat transfer and the background mechanics for the case of controlled cooling of steel rolling are summarized as [14]:

- The flow rate or jet velocity: effect of flow pattern
- The fluid temperature: the effect of sub-cooling
- The surface temperature: the effect of superheating
- The speed of surface motion

In the case of cryogenic machining, the second parameter cannot be separately controlled. Experiments need to be designed to help understand the boiling heat transfer on the machined surface of the workpiece during cryogenic machining, in order to properly assess the cooling effect.

2.3 Sustainability concerns in cryogenic machining

Liquid nitrogen is environmentally clean, toxic-free and safe. It is favored from the environmental and societal aspect, as it does not pollute the environment or cast threat to operators' health. When machining hard materials, cryogenic machining often offer better tool-life and surface finish compared to conventional flood cooling and other coolant alternatives. Also, it has a great potential to improve the surface integrity of finished products with improved functional performance and/or greater product life [11].

On the other hand, due to the much higher price of liquid nitrogen compared to other coolant of same volume, the economic performance of cryogenic machining has been questioned. Furthermore, dimensional tolerances of machined product and frostbite threat are of concerns, too [15]. The advantages and concerns of cryogenic machining are summarized in Table 1 below.

Table 1: Reported advantages and potential disadvantages of cryogenic machining

	Reported Advantages	Potential Disadvantages
Cost	Higher cutting speed / better tool-life	Coolant cost
Product Quality	Better surface integrity	Dimensional accuracy
Environment / society	Clean operation environment	Frostbite threat

3 DESIGN OF EXPERIMENT SETUP

A significant effort is devoted to temperature measurement on liquid nitrogen cooled surface. At this preliminary stage, the focus is to build a valid temperature measurement system for

the cryogenic machining scenario with a measurement tool described as follows.

3.1 Difficulties of temperature measurements in cryogenic machining

There were difficulties with the targeted measurements. First, the cryogenic temperature range limited the types of temperature measurement devices used. The thermocouples are chosen for wide temperature range coverage, but the working ranges involved is non-linear, thus simple integrated solutions are made impossible.

Another difficulty is the high cooling rate involved. The time of the cooling period will be in milliseconds. Infrared cameras on the market have a limited frame rate and a relatively long integration time. Several measurements of different temperature range taken to cover the wide temperature range would further degrade its performance over the dynamic target. While it is desirable to have a direct measurement of the entire temperature field, infrared cameras available now are not fast enough to capture the rapid temperature change it would have encountered under cryogenic machining conditions. The response time of thermocouples would depend on their bead size. Typically, the smaller the size is, the faster it would respond to the temperature change.

A further issue is the small scale involved. The material deformation zone and cutting region involved in machining are naturally sub-millimeter size. Also, due to the very short time involved, the cryogenically-cooled layer on the machined surface will be very shallow, which is estimated to be also sub-millimeter size.

3.2 Electronic system

The proposed solution is to use an ultra-thin thermocouple, coupled with a high bandwidth signal amplifier and a high speed data acquisition system. The captured voltage data will be mapped to the standard thermocouple table [16] to give the corresponding temperature reading, which will overcome the problem of non-linear behavior. The thermocouples used in experiments are Omega® CHAL-001 and CHAL-0005 K-type thermocouples, with a wire diameter of 25 μ m and 13 μ m, respectively. The bead diameters are measured to be around 60 μ m and 30 μ m, respectively. K-type thermocouple is selected due to its wide temperature range. The signal amplifier is based on Analog Devices® AD8421BRZ instrumentation amplifier, which gives a 3dB bandwidth of 2MHz at the gain of 100. The signal amplifier has a \pm 7V power supply unit built with voltage regulated from a lithium battery source and rail splitting circuits. The data acquisition unit used is National Instruments® NI USB-6366 USB-interfaced simultaneous data acquisition (DAQ) system, which provides a maximum sampling rate of 2MHz per channel. Matlab® codes are generated for data processing.

The DAQ system has a rated maximum noise of 1.3mV at the selected scanning range of \pm 5V. The power supply ripple noise is too low to be measured by the DAQ unit, as it is overwhelmed by the native noise of the DAQ unit. The circuit schematics of the signal amplifier is shown in Figure 3, though the components for the passive electromagnetic interference (EMI) filter are altered to permit a cutting frequency at 2.35MHz. The loaded noise recorded by the DAQ unit is 30mV peak-to-peak. The accuracy of the system is at worst around \pm 4°C. It should be noted that the electrical routing of the system is critical to its performance. Along with proper circuit routing, surface mounting devices (SMD) are

used for the signal amplifier to achieve desirable performance. Shielded cables are used between each two devices of the system.

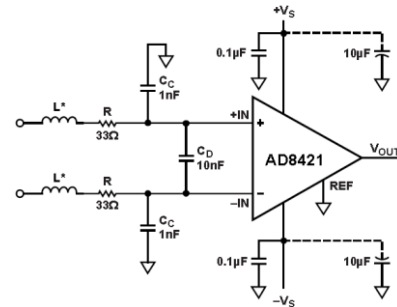


Figure 3: Signal amplifier circuit schematic [17].

Due to the small diameter, the thermocouple will show significant resistance, which is measured to be 670 Ω for 25 μ m diameter thermocouple with 30cm leads and 1250 Ω for 13 μ m diameter thermocouples with 20cm leads. To overcome the significant signal drifting introduced by the resistance, an amplifier chip with low offset voltage and small input bias current is needed, along with large current return resistors which are not shown in the schematics. This is one of the critical reasons why AD8421BRZ is chosen in this application. And, the commonly seen thermocouple breakage detection design is abandoned to reduce signal drifting. Also, care must be taken in not limiting the bandwidth due to the resistance of the thermocouple when designing the EMI filters.

3.3 Physical setup of preliminary tests

The two preliminary phases of the experiments on temperature measurement are on static surface. The liquid nitrogen jet is pumped from a 1MPa pressurized liquid nitrogen tank, and a plain round nozzle with an opening diameter of 3.18mm was used.

The first phase of the experiment is to test the capability of the high speed wide range temperature measurement system built, and was aimed at gaining some preliminary understanding of the boiling effects. The thermocouple is taped on a 1mm thick low density polyethylene (LDPE) strip, while the joint is exposed. The properties of common LDPE plastics [18] are summarized in Figure 4. The liquid nitrogen jet is aimed at 15° angle from the strip plain.

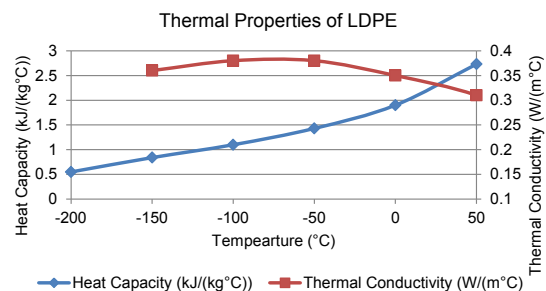


Figure 4: Common thermal properties of LDPE plastics [18].

The second phase of the experiments is on a 2011-T3 aluminum test block (specimen), and its dimensions are summarized in Figure 5.

The 12.7 mm diameter hole is used for clamping the test block. The small V-shape opening with a width of 4.75 mm

and at an angle of 11° is to simulate the geometric features of TPG43X insert doing orthogonal cutting, which is the typical setup used in the lab [19]. The geometry of the upper surface is the same as the flank surface of the insert, and the lower surface of the opening is to simulate the machined surface on a workpiece. To embed the thermocouple, a micro groove is machined on the surface of the bottom block, facing the opening. It is 2 mm away from the tip of the opening. Its dimension is measured using a Zygo® white light interferometer. The groove is trapezoid shaped, with the opening size of $60\ \mu\text{m}$, the bottom size of $10\ \mu\text{m}$ and the depth of $70\ \mu\text{m}$, as shown in Figure 6. Two larger notches are made at the groove edge end of the block.

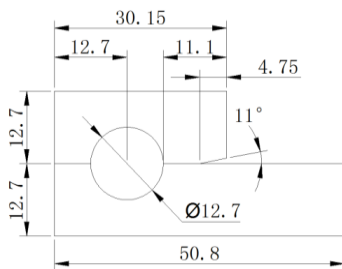


Figure 5: Dimensions of the aluminum test block, units in mm.

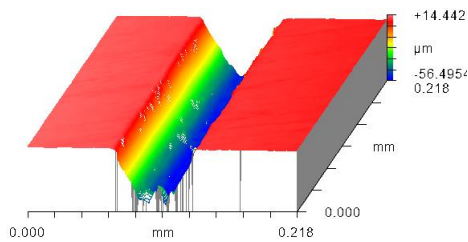


Figure 6: Measured groove dimensions.

The groove is filled with a thermal compound, which has a heat conductivity of $8.5\text{W}/(\text{m}^\circ\text{C})$. Then, the thermocouple is placed in to the groove by tensioning it with small downward forces around the two notches. Then, the setup is checked again to make sure the thermocouple is in place. It sits on top of the compound, slightly below the block surface. The bead is difficult to control and it may sometimes extend out of the groove, but within $20\ \mu\text{m}$ height, as shown in Figure 7.

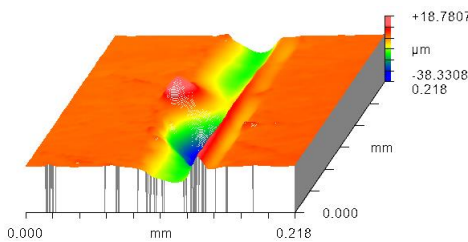


Figure 7: The bead extending out of the surface.

The liquid nitrogen jet is aimed at almost parallel to the lower surface of the V-shape opening. And, the nozzle tip is placed approximately 15mm away from the tip of the V-shape groove, which is the typical distance from the nozzle to the tool tip in flank-side cryogenic application of machining experiments.

4 PRELIMINARY EXPERIMENTAL RESULTS

The sample rate of data acquisition is 1MHz. The collected data are processed with Matlab® codes. Zero-drift compensation, cold joint compensation, moving average filtering of every ten samples and temperature mapping are performed in sequence. Each phase of experiments was performed five times. The results shown in the figures below are one of the five datasets, and the experiments showed good repeatability.

4.1 Results from the LDPE plastic strip

The measured surface temperature of LDPE plastic strip is shown in Figure 8.

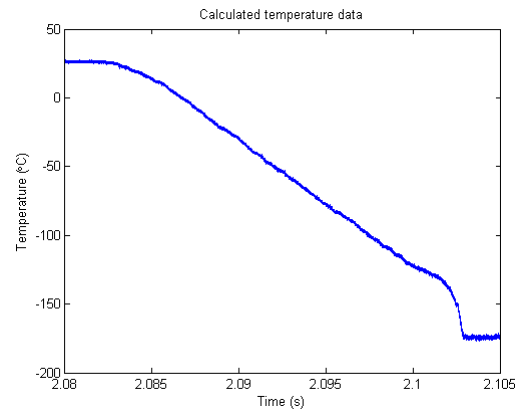


Figure 8: Measured temperature on the surface of LDPE under liquid nitrogen jet

It is interesting to find two distinguishing parts of the temperature curve. The stable part of the slow cooling section is taken out and least square polynomial fitting is applied. The data showed good fitting with 2nd order or above polynomial curves, as shown in Figure 9. The average cooling rate during this region is calculated by a first order polynomial fitting.

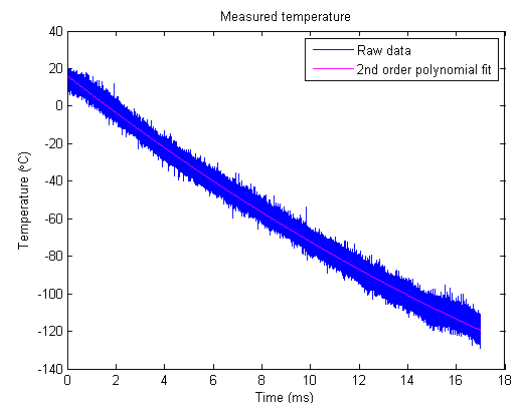


Figure 9: Temperature curve of the slow cooling region.

The stable part of the rapid cooling section is taken out and the above-mentioned process was applied, too. The results are shown in Figure 10. Summarizing the five data sets, the cooling rate of the slow cooling zone was $8.5\pm 0.5^\circ\text{C}/\text{ms}$, and the cooling rate of the rapid cooling zone was $65\pm 15^\circ\text{C}/\text{ms}$. The transition from slow cooling zone to rapid cooling zone occurs at $-140\pm 10^\circ\text{C}$. Stable temperature is $-181\pm 3^\circ\text{C}$.

Cooling rate within the rapid cooling section, and the transition temperature are not very stable among the five tests, but this agrees with the typical behavior of transition boiling.

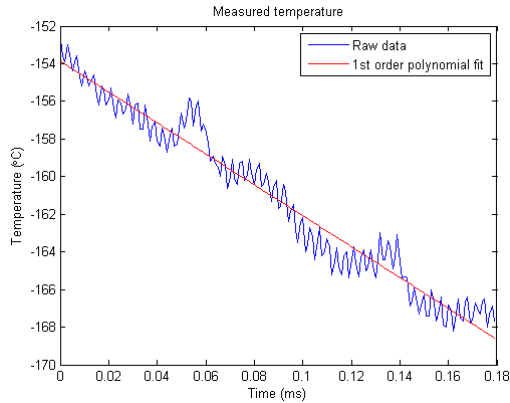


Figure 10: Temperature curve of the rapid cooling region.

4.2 Results from the aluminum test block

The measured surface temperature of aluminum test block which is described in detail in Section 3.3 is shown in Figure 11. The slow and rapid cooling sections are clearly identified. They are processed in a similar way as mentioned in Section 4.1. The measured cooling rate of the slow cooling zone was approximately $0.4 \pm 0.1^\circ\text{C/ms}$, and the cooling rate of the rapid cooling zone was $8.5 \pm 1.0^\circ\text{C/ms}$.

Condensed moisture forms water film and ice on the aluminum block surface. It was difficult to properly clean the test zone due to the congested geometry and fragility of the thin thermocouples. The measured results suggest cooling rate was one order of magnitude lower than the corresponding values shown in Section 4.1, for slow cooling and rapid cooling, respectively. This might be due to the combined effect of altered geometry, different materials and moisture condensing, while only the first two are designed variables.

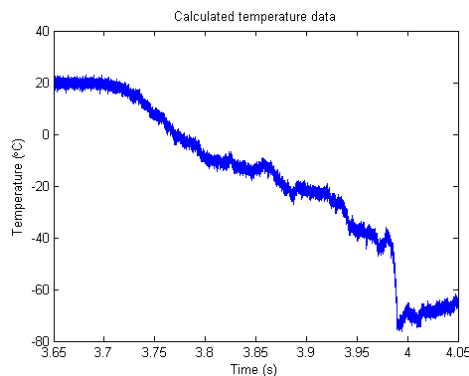


Figure 11: Measured temperature on the surface of aluminum test block under liquid nitrogen jet.

5 DISCUSSION AND FUTURE WORK

5.1 The heat transfer in cryogenic machining

A high speed wide range temperature measurement system is built and validated on two static scenarios. The two cooling sections with significantly different cooling rates suggest the

transition from the initial film boiling to the developed transition boiling, and potentially nucleate boiling, which are described in the Nukiyama Curve. The findings can be summarized, for the cases of cryogenic machining with liquid nitrogen jet applied on the flank surface, as follows.

The heat transfer on the machined surface of the workpiece is significantly influenced by the surface temperature and ultimately the surface super heating. When the super heating is significant, film boiling occurs and the heat flux will be relatively low. And, when the surface is cooled down, transition boiling and nucleate boiling may occur, which introduce much higher heat flux. The moving workpiece is subject to cooling from liquid nitrogen flow for a very limited amount of time, and a higher heat flux is often preferred, judged according to the magnitude of cooling rate measured.

The low heat flux during film boiling is due to the separation of coolant and hot surface by the vapor film. Surface motion and certain flow pattern would help the coolant penetrate the vapor film. The future direction is targeted at finding proper parameters that could maximize the rapid cooling section during cryogenic machining.

Unlike the machined surface, the cutting tool is static and is exposed to coolant flow for a prolonged time. Its flank side surface temperature would be closer to the coolant temperature, thus the different superheating effects need to be considered in the thermal analysis.

5.2 An overview at the sustainability concerns

To achieve truly sustainable manufacturing in cryogenic machining applications, one must consider all the aspects involving both process sustainability and product sustainability, as summarized in Figure 12.

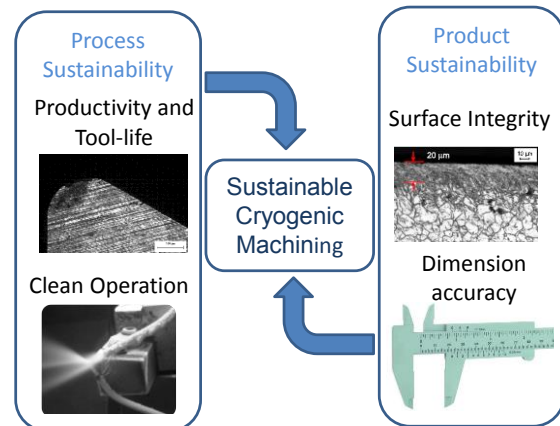


Figure 12: Achieving sustainable cryogenic machining.

As mentioned in Section 2.3, the major sustainability concerns of cryogenic machining are mostly due to the excessive use of liquid nitrogen. High flow rate of liquid nitrogen leads to a high consumption, which contributes to the problem of significant coolant cost. Instead of cooling the cutting zone only, the abundant amount of liquid nitrogen significantly reduces the temperature of the bulk part of the workpiece and the machine tool, causing dimension errors. Furthermore, the frozen workpieces and machine tools are at such a low temperature that they cannot be handled without proper protection equipment, and such low temperature is a

frostbite threat to the operators. The splashing liquid nitrogen streams are also hazardous frostbite potentials.

These issues can be solved by a proper application of cryogenic machining. The part need to be cooled is only the cutting zone, which includes the tip of the cutting tool and the surface layer on the workpiece. Thus, cooling of other parts in the system could be considered as a waste. The preliminary study showed that the exposure time and flow conditions are the major influencing factors of the cooling capacity in cryogenic machining applications. Thus, it is implied that a redundant amount of cooling media is not necessary here.

This indicates the necessity of applying cryogenic machining in the way that only the necessary amount of coolant should be applied, in order to minimize its negative impacts in economic, environment and societal aspects. While only the sufficient amount of liquid nitrogen is supplied to the cutting zone, the total consumption of the costly coolant may be greatly reduced. And the splashing of the cryogenic flow will be minimized. The cooling of the bulk part of the workpiece and the machine tool could be greatly reduced, thus the dimensional accuracy and frostbite threat would not be a problem anymore. Instead, the product quality might be improved [7][11].

5.3 Future Work

With proper understanding of the cooling phenomena in cryogenic machining, one could properly set the flow rate and nozzles used. From the sustainability point of view, the application of a proper amount of liquid nitrogen could be achieved as opposed to using an excessive amount non-productively. And such a savings would benefit the manufacturing operations in implementing the cryogenic machining processes by making a convincing case for economic sustainability, in addition to the well-proven environmental and societal sustainability elements.

6 ACKNOWLEDGMENTS

The authors would sincerely appreciate Mr. Charles Arvin's help in preparing the experiments.

REFERENCES

- [1] Byrne, G., Scholta, E., 1993, Environmentally Clean Machining Processes - A Strategic Approach, *CIRP Annals Manufacturing Technology*, 42: 471-474.
- [2] Hong, S.Y., Zhao, Z., 1999, Thermal Aspects, Material Considerations and Cooling Strategies in Cryogenic Machining, *Clean Technologies and Environmental Policy* 1: 107-116.
- [3] Sutherland, J.W., Kulur, V.N., King, N.C., Turkovich, B.F., 2000, An Experimental Investigation of Air Quality in Wet and Dry Turning, *CIRP Annals Manufacturing Technology*, 49: 61-64.
- [4] Lu, T., Shuaib, M., Rotella, G., Feng, S.C., Badurdeen, F., Dillon, O.W., Rouch, K.E., Jawahir, I.S., 2013. Sustainability Evaluation of Manufacturing Processes Using a Metric-Based Process Sustainability Index (ProcSI): Part I: Development of a Comprehensive Methodology, *Journal of Cleaner Production*, submitted.
- [5] Lu, T., Shuaib, M., Rotella, G., Feng, S.C., Badurdeen, F., Dillon, O.W., Rouch, K.E., Jawahir, I.S., 2013. Sustainability Evaluation of Manufacturing Processes Using a Metric-Based Process Sustainability Index (ProcSI): Part II: Method Applications and Validation. *Journal of Cleaner Production*, submitted.
- [6] Oxley, P.L.B., 1989, *The Mechanics of Machining: An Analytical Approach to Assessing Machinability*, Ellis Horwood, Chichester.
- [7] Umbrello, D., Rotella, G., 2012, Experimental Analysis of the Mechanisms Related to White Layer Formation during Hard Turning of AISI 52100 Bearing Steel, *Materials Science and Technology*, 28(2): 205-212.
- [8] Yue, Y., Sun, J., Gunter, K.L., Michalek, D.J., Sutherland, J.W., 2004, Character and Behavior of Mist Generated by Application of Cutting Fluid to a Rotating Cylindrical Workpiece, Part 1: Model Development, *Journal of Manufacturing Science and Engineering*, 126: 417-425.
- [9] Sun, J., Ju, C., Yue, Y., Gunter, K.L., Michalek, D.J., Sutherland, J.W., 2004, Character and Behavior of Mist Generated by Application of Cutting Fluid to a Rotating Cylindrical Workpiece, Part 2: Experimental Validation, *Journal of Manufacturing Science and Engineering*, 126: 426-434.
- [10] Li, X., 1996, Study of the Jet-Flow Rate of Cooling in Machining Part 1. Theoretical Analysis, *Journal of Materials Processing Technology*, 62: 149-156.
- [11] Hong, S.Y., Ding, Y., 2001, Cooling Approaches and Cutting Temperatures in Cryogenic Machining of Ti-6Al-4V, *International Journal of Machine Tools & Manufacture*, 41: 1417-1437.
- [12] Nukiyama, S., 1966, Maximum and Minimum Values of Heat Q Transmitted from Metal to Boiling Water under Atmospheric Pressure, *International Journal of Heat Transfer*, 9: 1419-1433.
- [13] Auracher, H., 2003, Some Remarks on the Nukiyama Curve, *JSME TED Newsletter*, 41.
- [14] Chen, S., Tseng, A., 1992, Spray and Jet Cooling in Steel Rolling, *International Journal of Heat and Fluid Flow*, 13(4): 358-369.
- [15] Yasa, E., Alpagan, U., Pilatin, S., Colak, O., 2012, A Review on the Improvements in Machinability of Ti-6Al-4V, *Proceedings of the 10th Global Conference on Sustainable Manufacturing*, Istanbul, Turkey, Oct 30 - Nov 2, 790-795.
- [16] National Institute of Standards and Technology, 2012, NIST ITS-90 Thermocouple Database, available at: http://srdata.nist.gov/its90/main/its90_main_page.html
- [17] Analog Devices, 2012, AD8421: 3 nV/√Hz, Low Power Instrumentation Amplifier Data Sheet, available at: http://www.analog.com/static/imported-files/data_sheets/AD8421.pdf
- [18] Martienssen, W., Warlimont, H., 2006, *Springer Handbook of Condensed Matter and Materials Data*, Springer, New York.
- [19] Rotella, G., Lu, T., Settineri, L., Jawahir, I.S., 2012. Machining of AA7075 Aluminum Alloy: a Process Optimization for Sustainability. *Proceedings of the 10th Global Conference on Sustainable Manufacturing*, Istanbul, Turkey, Oct 30 - Nov 2, 501-506.